Int. J. Aquat. Biol. (2017) 5(6): 375-386
ISSN: 2322-5270; P-ISSN: 2383-0956
Journal homepage: www.ij-aquaticbiology.com

Original Article

Implications of white spot syndrome virus disease on DNA integrity, histology and biochemistry of *Procambarus clarkii* in Egypt

Haidan M. El-Shorbagy* , Salwa Abdelhamid Hamdi

Department of Zoology, Faculty of Science, Cairo University, 12613, Egypt.

Abstract: White spot syndrome virus (WSSV) is a widespread and highly pathogenic virus; that infects shrimp, crayfish and other crustaceans. The objectives of the present study were to investigate WSSV implications on some crayfish tissues, within light and sever stages of infections. Several parameters have been investigated including DNA integrity, oxidative stress, and histological changes in gills, muscles and hepatopancreas cells, using several techniques such as comet assay, DNA fragmentation assay, oxidative stress biomarkers estimation and histopathological examination. Specimens were divided into three groups according to the nested PCR results. Group I included healthy specimens whose tissues were all negative two-step PCR; Group II involved lightly infected specimens with positive two-step PCR. Group III included heavily infected specimens whose tissues were tested mostly positive one-step PCR. WSSV generates an increase in the different parameters of DNA damage (P<0.05) with abnormal histological features and notable reduction (P<0.05) of the endogenous scavengers in the tested tissues of the infected crayfish in comparison with the normal healthy ones. Furthermore, gills were found to be the most affected organ followed by muscle and finally hepatopancreas. These outcomes additionally demonstrated that comet test could profitably be utilized in genotoxicity evaluation protocols in aquatic invertebrates.

Article history:
Received 11 September 2017
Accepted 20 October 2017
Available online 25 December 2017

Keywords:
Comet assay
DNA damage
White spot virus
Oxidative stress

Introduction

Procambarus clarkii, the red swamp crayfish, is considered to be one of the largest invasive species in the Egyptian aquatic environment that entered fresh water at the beginning of 1980'th (Hamdi, 2011). Crayfish exists in hardy warm freshwater that is found in reservoirs, marshes, rice fields, rivers and slow flowing water. It may become a keystone species, affecting many components of the ecosystem inhabits and altering the nature of native plant and animal communities.

Arthropods lack the highly advanced adaptive immune system of vertebrates. Instead, they only depend on their innate immune system to fight the invading microorganisms (Hoffmann et al., 1999). Thus, their capability to live are at risk nowadays due to the infection with white spot syndrome virus (WSSV).

It is known to date that WSSV can infect >90 species of deca-pod and non-decapod crustaceans from natural aquatic environments (Sánchez-Martínez et al., 2007). For the past 16 yr, WSSV has been identified as a severe and devastating pathogen of the farmed shrimp worldwide (Ramos-Carreño et al., 2014), as it is implicated in a serious economic impact on the shrimp aquaculture industry due to 80 to 100% mortality within 3 to 10 days post-infection (Sablok et al., 2012). Moreover, many reports indicated that WSSV is capable of significant morbidity and mortality in crayfish as well (Edgerton, 2004; Jiravanichpaisal et al., 2004). This resulted in significant economic losses in many crayfish-producing farms. Interestingly, researches in other crustacean species have demonstrated that many infected animals do not die, instead, they may act as reservoirs for the pathogen in ecosystems (Sánchez-Martínez et al., 2007), as WSSV-infected crayfish caused severe disease in a feeder population when being used in the diets of zoo residents maintained at the National Zoological Park in Washington, D.C.,

*Corresponding author: Haidan Mostafa El-Shorbagy
E-mail address: haidan@sci.cu.edu.eg
DOI: https://doi.org/10.22034/ijab.v5i6.378

USA (Richman et al., 1997).

WSSV is a double-stranded DNA virus with a very steady genome, assigned to the new genus, *Whispovirus*, in the family Nimaviridae (Vlak et al., 2005). WSSV is 110–130×260–350 nm, trilaminar enveloped, and rod-shaped (van Hulten et al., 2001). Many symptoms can be distinguished after WSSV infection, such as white spots in the exoskeleton and epidermis, loose cuticle, rapid reduction in food consumption, enlargement and yellowing of the hepatopancreas (Hameed et al., 2001); swelling of bronchioles as a result of accumulation of fluid; thinning and delayed clotting of haemolymph (Chakraborty and Ghosh, 2014). In addition, tropism analysis of tissue from both wild-captured brooders and experimentally infected shrimp, showed that cuticular epithelium and subcuticular connective tissues, antennal gland and haematopoietic organ were the core object tissues for WSSV. While samples from the gills, pleopods, abdominal muscle, haemolymph, still need further diagnostic testing (Lo et al., 1997).

Although host-virus interaction has been one of the recent attentions in understanding WSSV pathogenesis (Rodríguez et al., 2012; Leu et al., 2013), to our knowledge, there are no previous histopathological or molecular studies concerning WSSV effects on different *P. clarkii* tissues. Under these circumstances, an investigation of DNA damage, biochemical and the pathological changes in WSSV-infected crayfish are subjects worth studying to shed more lights on the most target organs for viral replication, host mortality, the potential anti-WSSV applications and the viral risk assessments on the aquatic environment, which help controlling their prevalence.

Materials and Methods

Chemicals: All chemicals used were of analytical grade and purchased from Sigma-Aldrich (St. Louis, MO, USA). Kits for all biochemical parameters were purchased from Bio-diagnostic Company (Giza, Egypt). Other molecular kits are listed elsewhere.

Animals: Fifty adult female Crayfish, *P. clarkii*, approximately 20 g and 8 cm each, were captured from their natural environment Al-Ayat aquacurium, Giza, Egypt and maintained in the laboratory as previously described (Zou et al., 2003). Animals were collected according to the clinical signs to be: 20 WSSV-free (no white spots) and considered as negative control and 30 WSSV-infected crayfish (with white spots). The prevalence of WSSV was further tested by WSSV diagnostic two-step PCR using a piece of the walking legs as a PCR template source to distinguish healthy animals from infected one. All samples were put in crushed ice in insulated containers and brought to the laboratory for preservation prior to analysis. The exoskeleton was removed, and three parts excised from crayfish specimens (gills, muscles and hepatopancreas) were divided into three parts each. One part was homogenized in cold Hanks buffer then stored at -20°C for comet analysis. The second part was used to extract DNA and subjected to PCR assays to reconfirm WSSV prevalence in the tested tissues and to carry out DNA fragmentation and biochemical tests, while the third part was fixed in 10% formalin for further processing for histopathological examination.

Nested PCR analysis for WSSV: Tissues under test were used for DNA extraction using DNA mini-prep kit (Qiagen, Sigma) and DNA quality was tested using decapod gene 143F: TGCCTTATCAGCTNTCGATT GTAG, 145R: TTCAGNTTTGCAACCATACTTCC C (848 bp) (OIE, 2003). Diagnosis of different WSSV-infected stages was performed by nested PCR as described previously (Lo et al.,1996) using outer nested primers 146F1: ACTACTAACTTCAGCCTA TCTAG, 146R1: TAATGCGGGTGTAATGTTCTT ACGA (1447 bp), for the one-step PCR, and Inner nested primers 146F2: GTAACTGCCCCTTCCATC TCCA, 146R2: TACGGCAGCTGCTGCACCTTGT (941 bp) for the two-step PCR. Positive and negative controls were also included to avoid any false positive PCR results. DNA extracts from experimentally infected crayfish were used as a positive control where the WSSV inoculum was prepared as previously described (Wang et al., 2009), and was injected into the last abdominal segment of *P. clarkii* (2.6×10^7 virions per crayfish). One-step PCR was performed by one cycle of initially denaturation at 94°C for 4 min,

55°C for 1 min, 72°C for 2 min, followed by 39 cycles at 94°C for 1 min, 55°C for 1 min and 72°C for 2 min and finally, final extension at 72°C for 5 min. Then 10 µl of the PCR product from samples with negative results of one-step PCR were used as a template for the two-step PCR over the same 40 cycles described above. Cycling was carried out using Thermal Cycler (PTC-100™ thermal cycler, Watertown, MA, USA). The PCR products were separated by electrophoresis on 1% agarose gels, stained with 2% ethidium bromide and visualized by UV trans-illuminator (Stratagene, USA). Tested specimens were divided into three groups based on nested PCR results. Group I comprised specimens whose tissues were all two-step PCR negative, Group II comprised lightly infected specimens (GP.II) which had at least some tissues positive after re-amplification and Group III comprised heavily infected specimens (GP.III) whose tissues tested one-step PCR positive.

Comet analysis: Comet technique was carried out for 7 animals for each group, according to Singh et al. (1998) with some modifications. Cell suspension (10 µl), previously homogenized with Hanks buffer was mixed with 75 µl of low melting agarose (0.5% in PBS). The mixture was spread on 1% agarose pre-coated slides. The slides were immersed in cold lysed buffer (2.5 M NaCl, 100 mM EDTA, 10 mM Tris, pH 10, to which 1% Triton X-100 and 10% DMSO were freshly added) for 24 hours at 4°C in dark. Then they were placed in electrophoresis chamber containing the alkaline electrophoresis buffer for another 20 minutes. The electrophoresis was carried out for 20 minutes at 300 mA and 25 V. Then neutralization was done using 0.4 m Tris (pH7.5). The slides were stained with ethidium bromide 20 µg/ml. DNA fragment migration patterns of 50 cells for each animal were examined using a fluorescent microscope (with excitation filter 420-490 nm (issue 510 nm) linked to a CCD camera. Comet Assay IV software (Perceptive Instruments, Suffolk, UK), was used to assess tail moment, DNA% in tail and tail length of DNA damage, at 400X.

DNA-laddering assay: According to the standard protocol described by Sriram et al. (2010), tested tissues were homogenized in cold lysis buffer containing 10 mM Tris HCl, pH 7.4, 10 mM EDTA, and 0.2% TritonX-100. Then incubated with 0.6 µg/mL proteinase K at 50°C overnight and consequently with RNase A to a final concentration 100 µg/mL at 37°C for one hour. Extraction with phenol chloroform isoamyl was carried out, and DNA in the aqueous phase was precipitated by 25 µL (5 M) Sodium chloride and 100% isopropanol at -20°C. The concentration of the extracted DNA was measured and 5 µg from each sample was detected by migration on a 1.5% ethidium bromide-treated agarose gel through electrophoresis at 80 Volt (power supply Biorad, Hercules, CA, USA, Model 200/2.0). Finally, fragmented DNA could be visualized under UV transillminator (Stratagene, La Jolla, CA, USA).

Oxidative stress markers: Tissue samples of gills, muscle, and hepatopancreas were homogenized in a 10% (w/v) in cold Tris HCL buffer 0.1 mM pH 7.4 at 4°C. The homogenates were centrifuged at 10000g for 15 min at 4°C and supernatants were immediately used for determining glutathione peroxidase (GPx), catalase (CAT) and superoxide dismutase (SOD) activities according to manufacturer's instructions.

Glutathione peroxidase (GPx) activity: According to Paglia and Valentine (1967), GPx activity was measured indirectly upon the oxidation rate of NADPH. The reaction depends on the reduction of peroxides in which oxidized glutathione (GSSG) is produced and recycled to its reduced state by glutathione reductase. The oxidation of NADPH to NADP+ is accompanied by a decrease in the absorbance at 340 nm (A340) providing a spectro-photometric means for monitoring GPx enzyme activity. The rate of the decrease in the A340 is directly proportional to the GPx activity in the sample. A blank without homogenate was used as a control for non-enzymatic oxidation of NADPH upon addition of hydrogen peroxide in 0.1 M Tris buffer, pH 8.0. Enzyme activity were expressed as unit/g tissue.

Superoxide dismutase (SOD) activity: SOD activity was measured using Nishikimi et al. (1972) method which is based on its ability to inhibit nitro blue tetrazolium (NBT) reduction by xanthine-xanthine oxidase after the addition of superoxide dismutase.

Table 1. DNA damage represented as Tail length, %DNA in tail and Tail moment in three tissues (hepatopancreas (H), muscles (M) and gills (G)) within control (Gp.I), lightly infected (Gp.II) and heavily infected (Gp.III) crayfish.

Parameter	Tissue	Experimental group		
		I	II	III
Tail length (µm)	H	0.30 ± 0.04^{Cc}	0.98 ± 0.03^{Bc}	2.68 ± 0.14^{Ac}
	M	0.32 ± 0.03^{Cb}	1.97 ± 0.05^{Bb}	3.06 ± 0.21^{Ab}
	G	0.34 ± 0.09^{Ca}	2.53 ± 0.08^{Ba}	5.41 ± 0.51^{Aa}
%DNA in tail	H	1.16 ± 0.13^{Cc}	1.98 ± 0.21^{Bc}	2.51 ± 0.11^{Ac}
	M	1.27 ± 0.16^{Cb}	2.12 ± 0.28^{Bb}	3.03 ± 0.29^{Ab}
	G	1.61 ± 0.13^{Ca}	2.98 ± 0.15^{Ba}	3.65 ± 0.29^{Aa}
Tail moment	H	0.003 ± 0.001^{Cc}	0.019 ± 0.001^{Bc}	0.067 ± 0.004^{Ac}
	M	0.004 ± 0.001^{Cb}	0.063 ± 0.001^{Bb}	0.094 ± 0.014^{Ab}
	G	0.005 ± 0.002^{Ca}	0.089 ± 0.001^{Ba}	0.198 ± 0.023^{Aa}

Results are expressed as mean ±SE. In each row, the mean values marked with the same superscript Capital letters are similar (insignificant, $P>0.05$) whereas those with different ones are significantly differed ($P<0.05$). In each column, the mean values marked with the same superscript Small letter are similar (insignificant, $P>0.05$) whereas those with different ones are significantly differed ($P<0.05$). $P>0.05$: insignificant effect; $P<0.0001$: significant effect at $\alpha=0.0001$.

SOD activity was expressed as unit/g tissue.

Catalase (CAT) activity: In Aebi (1984) method , the catalase activity was measured by measuring the breakdown of H_2O_2 where CAT reacts with a known quantity of H_2O_2 and stopped after exactly 1 min using CAT inhibitor. In the presence of peroxidase, the remaining H_2O_2 reacts with 3, 5-dichloro-2-hydroxybenzene sulfonic acid and 4- aminophenazone forming a that can be measured spectrophotometrically at 510 nm. Thus, the color intensity is inversely proportional to the amount of CAT in the tested sample. Results were expressed as U/min.

Histological examination: For pathological studies portions of gills, muscles and hepatopancreas tissues were fixed in neutral buffered formalin (10%) overnight, washed with tap water, dehydrated using grades of ethanol (70%, 90%, 95%, and 100%) and followed by clearing the samples in two changes of xylene. Then impregnated with two changes of molten paraffin wax, embedded, and blocked out. Samples were sliced to 3-4 µm thickness. The obtained tissue sections were collected on glass slides, dewaxed with xylene and rehydrated through a descending alcohol series and finally were stained with haematoxylin and eosin (H&E) (Bancroft et al., 1996). The stained sections were evaluated using light microscopy (U-III Multi-point Sensor System; Nikon, Tokyo, Japan) and photographed using IS_Capture Camera system.

Statistical Analysis: The present data were analysed by Statistical Package for the Social Sciences (SPSS) version 15. Two-ways ANOVA was applied to test the effect of infection, type of tissue and their interaction on the studied parameters. Duncan's test of homogeneity was used to test the similarities between the studied groups. All the results were expressed as a mean ± standard error of mean (SEM).

Results

Clinical Signs: White spots or patches embedded in the exoskeleton and loose cuticle are the principle clinical signs of WSSV-infected crayfish (Fig. 1A, B). Other signs may include whiteness of body and appendages.

SSV nested PCR detection: Samples with successful amplicons (1447 bp) from one-step PCR have been considered as Gp.III (heavily infected-crayfish), while those showed negative results have been subjected to two-step PCR, yielding two groups either contain positive amplicons that showed two bands (1447 and 941bp) which considered as Gp.II (lightly infected-crayfish) or negative samples that considered to be (Gp.I) healthy crayfish (Fig. 2).

Comet assay: Significant difference ($P<0.05$) in DNA damage could be detected between lightly infected (Gp.II) and their control (Gp.I). All the heavily infected tissues (Gp.III) (muscles (M), gills (G) and

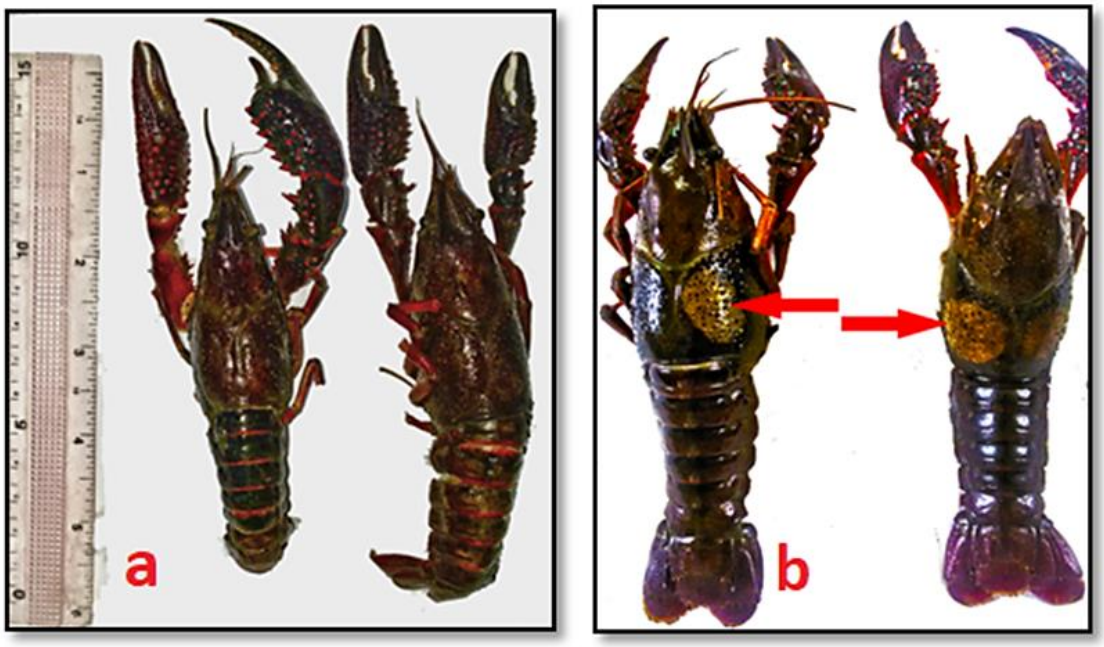

Figure 1. External observations of *Procambarus clarkii* (a) healthy *P. clarkii*, (b) WSSV- infected *P. clarkia* showing White spots in the carapace.

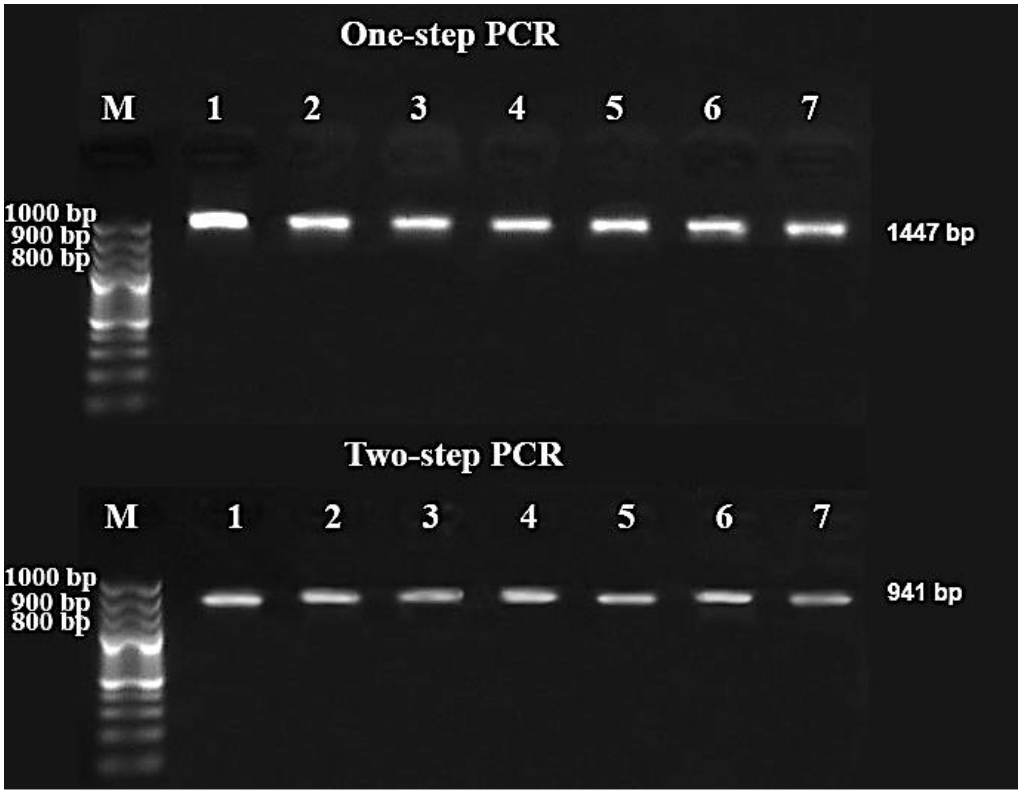

Figure 2. Representative photo showing PCR product of one-step PCR (1447bp) and two-step PCR (1447and 941bp), where (M): DNA marker. Lanes (1-2): gill (G), lanes (3-4) muscle (M), lanes (5-6) hepatopancreas (H) and lane (7): positive control.

hepatopancreas (H)) showed statistically significant increase ($P< 0.05$) in all DNA damage parameters (tail length, %DNA in tail and tail moment) in comparison with their corresponding tissues in Gp.I and Gp.II as shown in Table 1. Within Gp.III, gill showed the highest DNA damage between all tested tissues while hepatopancreas revealed the lowest one at ($P< 0.05$) (Fig. 3).

DNA–Ladder assay: The present findings revealed slight smear in all tested tissues within GP.II

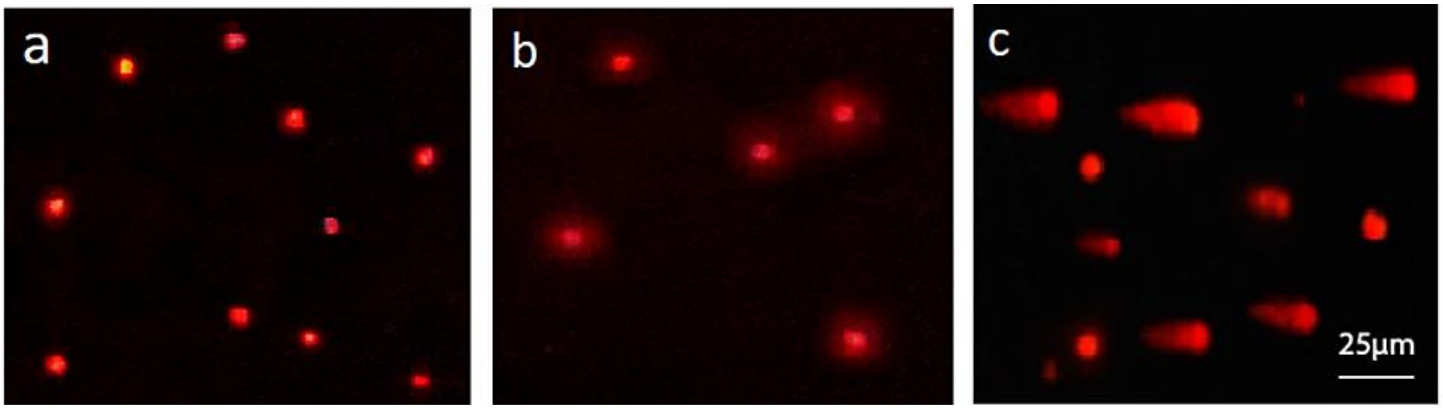

Figure 3. Representative photo of damaged DNA in light WSSV-infected *Procambarus clarkii* (b), heavy WSSV-infected *P. clarkii* (c) and compared with undamaged DNA (a) (400X).

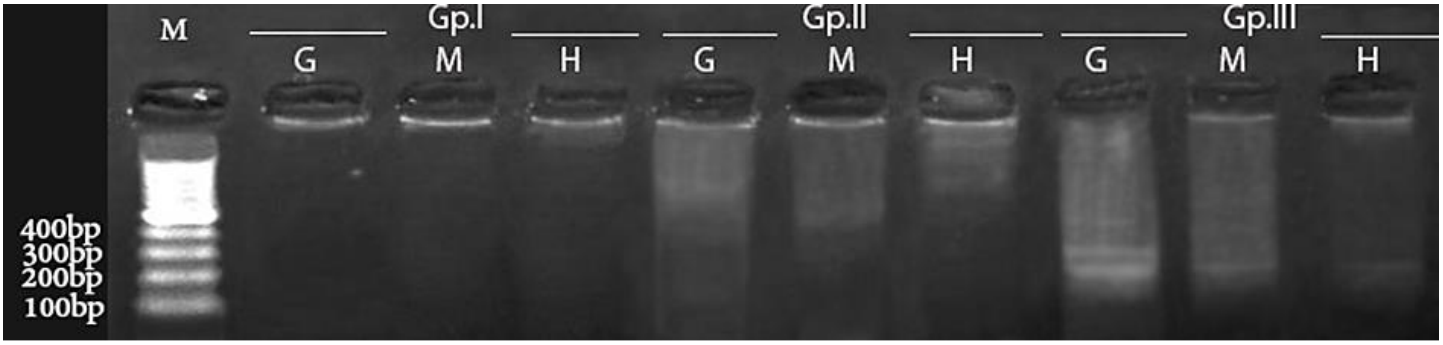

Figure 4. Representative photo showing smeared and laddered DNA laddering within lightly infected group (Gp.II) and heavily infected group (Gp.III) respectively, in the three tested tissues gill (G), muscles (M) and hepatopancreas (H) compared to the intact DNA of the healthy control group (Gp.I).

Parameter	Tissue	Experimental group			Effect of infection	Effect of tissue type	Effect of interaction
		I	II	III			
SOD (U/g tissue)	H	246.79±1.85^{Ca}	223.13±1.50^{Ba}	191.43±2.10^{Aa}	$F_{1,12}$=728.54, P<0.0001,	$F_{2,12}$=815.87, P<0.0001,	$F_{2,12}$=35.79, P<0.0001,
		---	(-9.58%) ^{P}	(-22.43%) ^{P}			
	M	289.01±5.43^{Cb}	257.99±1.52^{Bb}	207.01±4.35^{Ab}			
		---	(-10.73%) ^{P}	(-28.37%) ^{P}			
	G	390.83±6.45^{Cc}	333.78±1.78^{Bc}	262.73±1.20^{Ac}			
		---	(-14.60%) ^{P}	(-32.78%) ^{P}			
GPx (U/g tissue)	H	1025.57±2.79^{Ca}	977.93±1.22^{Ba}	841.86±6.04^{Aa}	$F_{1,12}$=858.96, P<0.0001,	$F_{2,12}$=3028.61, P<0.0001,	$F_{2,12}$=139.93, P<0.0001,
		---	(-4.65%) ^{P}	(-17.91%) ^{P}			
	M	1142.07±6.22^{Cb}	999.98±0.93^{Bb}	980.65±3.93^{Ab}			
		---	(-12.44%) ^{P}	(-14.13%)			
	G	1457.38±16.75^{Cc}	1233.23±1.59^{Bc}	1130.75±4.54^{Ac}			
		---	(-15.38%) ^{P}	(-22.41%) ^{P}			
CAT (U/min/g tissue)	H	56.26±2.82^{Cb}	44.24±0.63^{Bb}	36.05±0.22^{Ab}	$F_{1,12}$=197.03, P<0.0001,	$F_{2,12}$=2895.32, P<0.0001,	$F_{2,12}$=41.28, P<0.0001,
		---	(-21.38%) ^{P}	(-35.93%) ^{P}			
	M	32.14±0.89^{Ca}	26.47±0.33^{Ba}	23.83±0.49^{Aa}			
		---	(-17.62%) ^{P}	(-25.85%) ^{P}			
	G	118.67±1.64^{Cc}	93.95±0.16^{Bc}	76.52±1.12^{Ac}			
		---	(-20.84%) ^{P}	(-35.52%) ^{P}			

In each row, the mean values marked with the same superscript Capital letters are similar (insignificant, P>0.05) whereas those with different ones are significantly differed (P<0.05). In each column, the mean values marked with the same superscript Small letters are similar (insignificant, P>0.05) whereas those with different ones are significantly differed (P<0.05). P>0.05: insignificant effect; P<0.0001: significant effect at α=0.0001.

when compared to the negative control. WSSV induced apoptotic DNA fragmentation within GP.III expressed as 200bp and 250bp laddering in gill tissue, while muscle and hepatopancreas show only one band at 200bp (Fig. 4).

Histopathological Examination: Histopathological

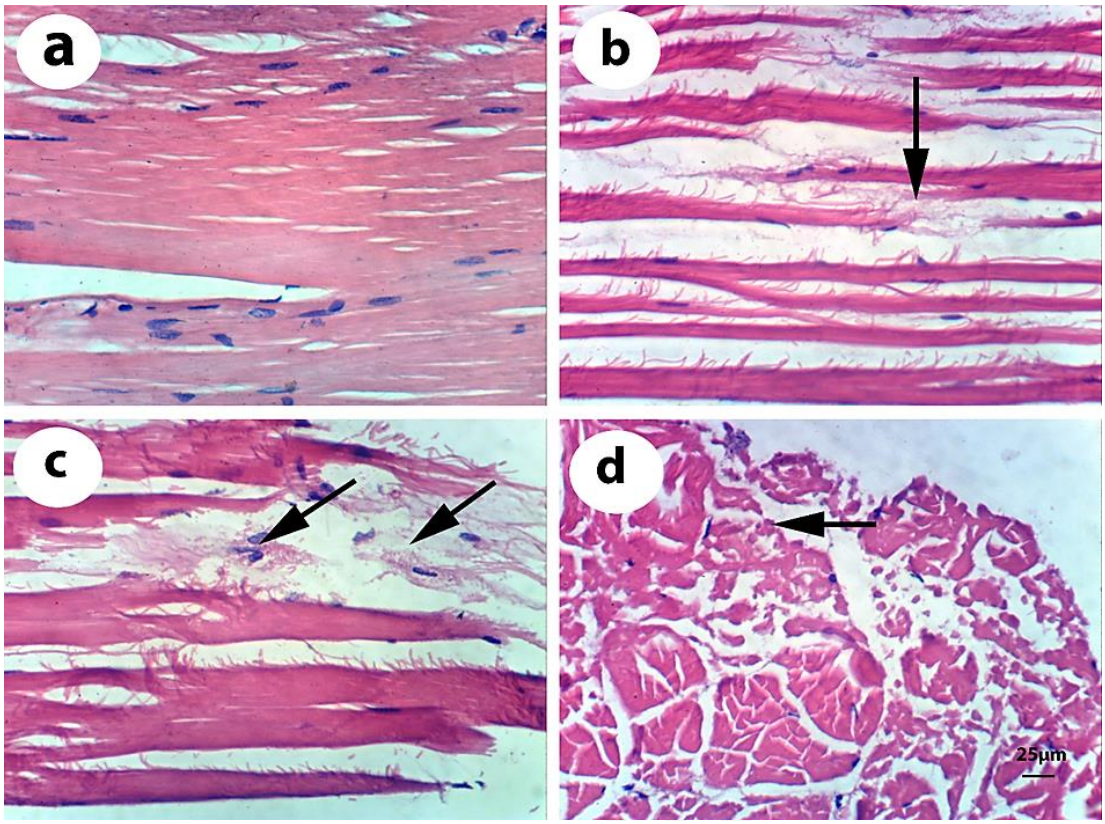

Figure 5. Photomicrograph of crayfish muscles represents: (a) control muscles showing no histopathological changes. WSSV-infected crayfish representing, (b) Gp.II showing intermuscular edema (indicated by arrow), (c) Gp.III showing: myolysis of focal myocytes, and (d) Zenker's necrosis of myocytes (indicated by arrows) (H&E).

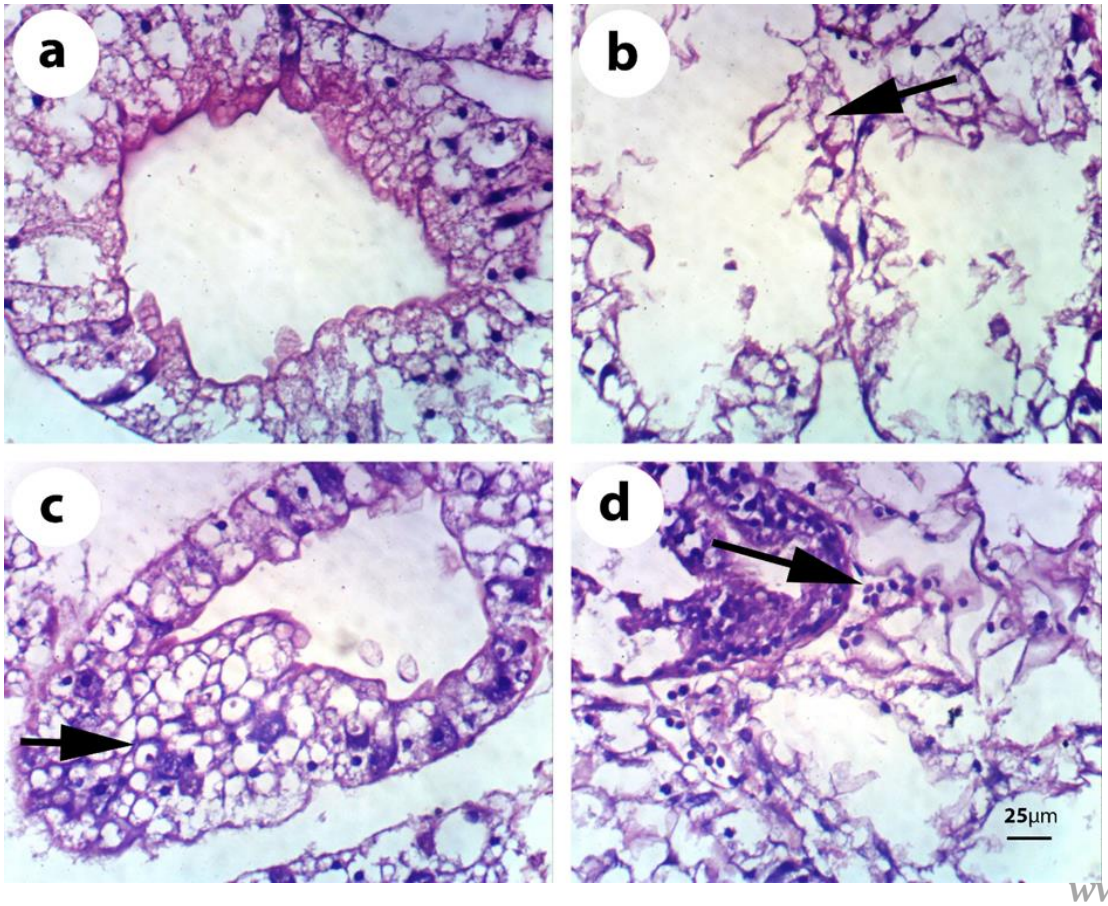

Figure 6. Photomicrograph of crayfish hepatopancreas tubules represents: (a) control group showing apparent normal hepatopancreas tubules. WSSV-infected crayfish representing, (b) Gp.II showing necrosis of cells of hepatopancreas tubules (indicated by arrow), (c) Gp.III showing: highly vacuolated cells and (d) inflammatory cells infiltration within necrotic cells (indicated by arrows) (H&E).

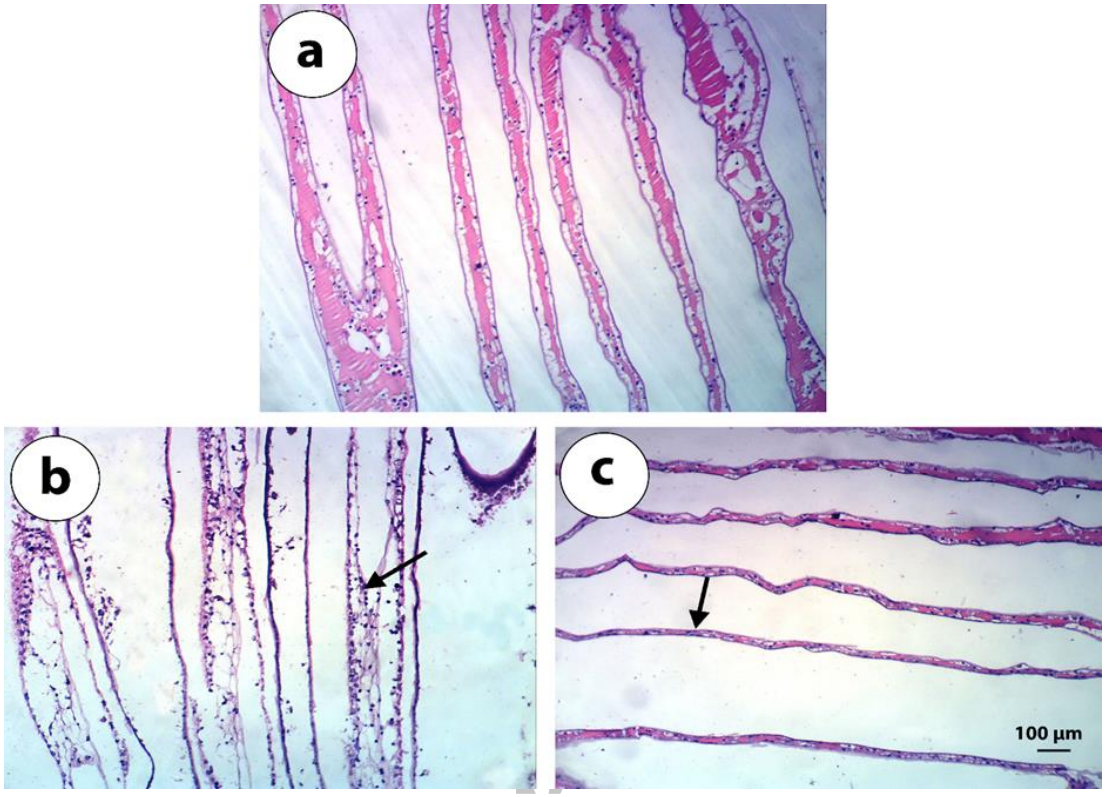

Figure 7. Photomicrograph of crayfish hepatopancreas tubules represents: (a) control group showing no histopathological changes. WSSV-infected crayfish representing, (b) Gp.II showing necrosis of gill lamellae (indicated by arrow) and (c) Gp.III showing: atrophy of gill lamellae (indicated by arrows) (H&E).

changes within control, Gp.II and Gp.III were evaluated. Several abnormal architectures were observed in gill tissue within Gp.II and Gp.III showing necrosis and atrophy of gill lamellae respectively (Fig. 5).

Alteration of muscle fibers including intermuscular edema within Gp.II, and myolysis of focal myocytes with Zenker's necrosis in Gp.III were clearly detected (Fig. 6). Moreover, necrotic cells of hepatopancreas tubules could be observed within Gp.II, while highly vacuolated cells and necrotic cells with inflammatory cell infiltration could be noticed only within GP.III (Fig. 7).

Oxidative stress markers: There was a significant reduction (P<0.05) in the levels of all measured endogenous enzymes SOD, GPX1 and CAT in Gp II and Gp III (Table 2). The reduction of anti-oxidant enzymes was parallel to the severity of the infections. Gills within Gp.III showed the most affected organ among all tested tissues for SOD and GPx levels (-32.78% and -22.41%) respectively, while the change in CAT activity was equally higher in gills and hepatopancreas (-35.52% and -35.93%, respectively) than in muscles tissues.

Discussion

In the present study, WSSV infected crayfishes have been randomly chosen according to the existence of clear white spots or patches embedded in their exoskeleton, and then tested to ensure WSSV infection and classified using 1 or 2-step PCR assay. These clinical signs were previously reported in different crustacean species infected with WSSV (Lo et al., 1996; Kasornchandra et al., 1998). The formation of white spot may be contribute to the accumulation of calcium salts within the cuticle as a result of the dysfunction of the integument results in the white spots formation(Wang et al., 1999).

White spot syndrome virus target the cells of ectodermal and mesodermal origin, including lymphoid organ, antennal gland, epidermis, gills, muscle and eye-stalk (Kou et al., 1998). According to comet assay, the present data declare that WSSV infection induced the highest DNA damage in gill cells followed by muscle and finally hepatopancreas within both the Gp.II and Gp.III in comparison with the normal healthy group (Gp.I). Indeed, the percentage of DNA in the tail (tail intensity) was found to be proportional to the frequency of DNA strand breaks (Olive et al., 1990). This is may be contributed to the increasing of the apoptotic rate in the late stage of infection due to the release of high viral copy numbers, that differ after post viral exposure from tissue to the other as indicated by Tan et al. (2001) who revealed that viral copy numbers were below the detectable levels during the first 12 h post-exposure, and that viral DNA was first detected 14 h post-exposure in gills and integument, while first detection was 22 h post-exposure in muscle tissue (Tan et al., 2001). Additionally, some reports investigated WSSV replication in several infected specimens, and it was particularly prevalent in gills, followed by muscle and finally hepatopancreas, it is in these organs that the virus most frequently appears and replicates (Kou et al., 1998, Shi et al., 2005). These in contrary with Sahtout et al. (2001) findings that revealed the highest number of apoptotic cells within gills then hepatopancreas and finally within muscle in black tiger shrimp, which may be due to the difference in crustaceans species (Sahtout et al., 2001). However, double stranded viral DNA can be distinguished from the host damaged DNA using comet test and DNA ladder assay by its heavy size (~300 kbp) which obligate viral DNA to be close to the nucleus rather than moving by the electrophoretic current as fragmented DNA in the damaged or lysed cells. Anyway, the GP.II revealed an extent of significant DNA damage and smeared DNA, this is may be contributed to the life-death struggle, in which virus intend to inhibit apoptosis in order to replicate in the early stage of infection, while the host defense system induce apoptosis to kill virus (Leu et al., 2013). Simultaneously, WSSV in Gp.III showed signs of late stage apoptosis, as shown by two different laddered bands in the tested infected tissues indicating that the extend of apoptosis is proportional to the severity of the infection, these data are in a harmony with the study of Sahtoot et al. (2001) on WSSV- infected *Penaeus monodon* who revealed that number of TUNEL positive cells present in gill, stomach, abdomen and muscle tissues increased with cumulative severity of infection, as determined by gross signs of white spots on the cuticle. However, this is a study of randomly captured crayfish, so it did not display whether the crayfish died rather due to WSSV infection or survived for longer because of the reduction in the apoptotic level. As apoptosis is initiated through two major pathways: the extrinsic pathway and the intrinsic pathway (Danial and Korsmeyer, 2004), we can postulate that the intrinsic pathway is that main way of WSSV induced apoptotic mechanism cause it initiated by signals arising within the cells such as survival factors depletion, DNA damage, viral infection, and oxidative stress as indicated by the present study.

Recently, some studies have reported that the infection with WSSV is accompanied with up-regulation of Zn-finger protein within crayfish haemocytes as previously reported by Zeng et al. (2009). The zinc-finger antiviral protein (ZAP) is a kind of zinc-finger protein which considered as a host factor that inhibits the replication of many viruses by preventing the viral mRNA accumulation in the cytoplasm. ZAP binds to the viral mRNA and recruits the cellular RNA degradation machinery to degrade the target RNA (Garcia and Damonte, 2007; Zhu and Gao, 2008). Du et al. (2012) reported that Zn-finger protein induced DNA double strand breaks, which may declare another possible mechanism of DNA-damage induced by WSSV in crayfish.

Knowing that Crayfish being often considered as a biological indicator species of the heavy metal pollution existing in the aquatic environment and by considering the findings of most studies that observed the highest concentrations of each metal were inside the hepatopancreatic tissue (Madigosky et al., 1991).

We cannot conclude that the resultant DNA damage could be due to metal accumulation as hepatopancreas reported the least DNA damage among tested tissues.

As WSSV is a lytic virus that replicates and assembles in the nucleus, resulting in lysis of the infected nuclei/cells thus the cells of the infected tissues may become severely damaged in the late stages of infection; that may cause organ dysfunctions, necrosis and perhaps leads to death (Kou et al., 1998, Leu et al., 2013). These implications could be further proved in the present study using histopathological examinations that demonstrated several abnormal architecture recording ascending scores of damages according to the severity of infections.

The observed histopathological changes including edema, Zenker's necrosis in muscle fibers and necrosis in gills and hepatopancreatic cells further confirmed WSSV mediated apoptosis in the tested tissue. The observed necrotic cells with inflammatory cell infiltration have been reported as indicators of the oxidative stress triggered by depletion of glutathione in these cells (Alarifi et al., 2013). The observed edema may attributed to the entry of solutes and water that resulted from the loss of membrane fluidity and function induced by oxidative stress (Galli et al., 2003).

WSSV-induced oxidative stress could be confirmed by the significant reduction of the antioxidant defense systems represented by SOD, GPx and CAT activities in respect to the negative control. These three anti-oxidant enzymes provide the first line defense against oxidative stress. Thus, the resultant reactive oxygen stress (ROS), which overwhelmed the antioxidant defenses causing DNA damage, is mostly caused by the hydroxyl radical (OH·) and superoxide anion radical (Hayes and Mclellan,1999). Therefore, further investigations of the possible changes in mitochondrial genes expression levels or the expression of genes related to the antioxidant defense mechanism should be studied.

The results presented here give some evidences to the prediction of the viral accommodation theory which states that when an active crayfish mechanism to accommodate fatal viral infection fails, they will show signs of cell death by apoptosis that explain the common persistence of viral infection in crayfish. Of interest, in some insect baculoviruses, viral infections would usually cause apoptosis unless blocked by specific genes that involved in the production of the Inhibitors of Apoptosis Proteins (IAP) (Clem et al., 1991), thus this might be the case. Anyway, more studies are essential to determine (IAP) genes in WSSV other than *P35* and *Iap* which are able to control apoptosis in a variety of eukaryotes (Clem et al., 1996), and whether it might activate apoptosis at some point during infection.

Conclusion: This is the first study that demonstrates the damaging effects of WSSV on DNA integrity, histopathological structure and endogenous defense antioxidant enzymes in different tested tissues of crayfish, especially gills which can be considered as a target organ for early detection of WSSV. From the present work, we can speculate that apoptosis may be the reason of death in crayfish with mortal viral infections and that it may be considered as an essential part of the adaptive tolerance process against viruses in crustaceans. Moreover, these findings declare that the comet assay had adequate sensitivity to detect the differences in the levels of DNA damage among different levels of infection within aquatic animals.

Acknowledgments

This work was supported by Faculty of Science-Cairo University. Authors would like to thank Prof. Dr. Koukap Abd_elazez Ahmed for her great help in slicing, staining, photographing and examining the histological specimens.

References

Aebi H. (1984). [13] Catalase in vitro. Methods in Enzymology, 105: 121-126.

Alarifi S., Ali D., Al-Doaiss A.A., Ali B.A., Ahmed M., Al-Khedhairy A.A. (2013). Histologic and apoptotic changes induced by titanium dioxide nanoparticles in the livers of rats. International Journal of Nanomedicine, 8(8): 3937-3943.

Bancroft J., Stevens A., Turner D. (1996). Theory and practice of histological techniques 4th Ed Churchill Living Stone, New York Edinburgh. Madrid, Sanfrancisco.

Chakraborty S., Ghosh U. (2014). White spot syndrome virus (WSSV) in crustaceans: an overview of host-pathogen interaction. Journal of Marine Biology and Oceanography, 31: 2.

Clem R., Hardwick J., Miller L. (1996). Anti-apoptotic genes of baculoviruses. Cell Death and Differentiation, 3(1): 9-16.

Clem R.J., Fechheimer M., Miller L.K. (1991). Prevention of apoptosis by a baculovirus gene during infection of insect cells. Science, 254(5036): 1388-1390.

Danial N.N., Korsmeyer S.J. (2004). Cell death: critical control points. Cell, 116(2): 205-219.

Do T.U., Ho B., Shih S.-J., Vaughan A. (2012). Zinc finger nuclease induced DNA double stranded breaks and rearrangements in MLL. Mutation Research/ Fundamental and Molecular Mechanisms of Mutagenesis, 740(1): 34-42.

Edgerton B.F. (2004). Susceptibility of the Australian freshwater crayfish *Cherax destructor albidus* to white spot syndrome virus (WSSV). Diseases of Aquatic Organisms, 59: 187-193.

Galli F., Ghibelli L., Buoncristiani U., Bordoni V., D'Intini V., Benedetti S., Canestrari F., Ronco C., Floridi A. (2003). Mononuclear leukocyte apoptosis in haemodialysis patients: the role of cell thiols and vitamin E. Nephrology Dialysis Transplantation, 18(8): 1592-1600.

Garcia C., Damonte E. (2007). Zn finger containing proteins as targets for the control of viral infections. Infectious Disorders-Drug Targets (Formerly Current Drug Targets-Infectious Disorders), 7(3): 204-212.

Hamdi S.A. (2011). Muscle and exoskeleton extracts analysis of both fresh and marine crustaceans *Procambarus clarkii* and *Erugosquilla massavensis*. African Journal of Pharmacy and Pharmacology, 5(13): 1589-1597.

Hameed A.S., Yoganandhan K., Sathish S., Rasheed M., Murugan V., Jayaraman K. (2001). White spot syndrome virus (WSSV) in two species of freshwater crabs (*Paratelphusa hydrodomous* and *P. pulvinata*). Aquaculture, 201(3): 179-186.

Hayes J.D., Mclellan L.I. (1999). Glutathione and glutathione-dependent enzymes represent a co-ordinately regulated defence against oxidative stress. Free Radical Research, 31(4): 273-300.

Hoffmann J.A., Kafatos F.C., Janeway C.A., Ezekowitz R. (1999). Phylogenetic perspectives in innate immunity. Science, 284(5418): 1313-1318.

Jiravanichpaisal P., Söderhäll K., Söderhäll I. (2004). Effect of water temperature on the immune response and infectivity pattern of white spot syndrome virus (WSSV) in freshwater crayfish. Fish and Shellfish Immunology, 17(3): 265-275.

Kasornchandra J., Boonyaratpalin S., Itami T. (1998). Detection of white-spot syndrome in cultured penaeid shrimp in Asia: Microscopic observation and polymerase chain reaction. Aquaculture, 164(1): 243-251.

Kou G.-H., Peng S.-E., Chiu Y.-L., Lo C.-F. (1998). Tissue distribution of white spot syndrome virus (WSSV) in shrimp and crabs. Advances in Shrimp Biotechnology, 267-271.

Leu J.-H., Lin S.-J., Huang J.-Y., Chen T.-C., Lo C.-F. (2013). A model for apoptotic interaction between white spot syndrome virus and shrimp. Fish and Shellfish Immunology, 34(4): 1011-1017.

Lo C.-F., Ho C.-H., Peng S.-E., Chen C.-H., Hsu H.-C., Chiu Y.-L., Chang C.-F., Liu K.-F., Su M.-S., Wang C.-H. (1996). White spot syndrome baculovirus (WSBV) detected in cultured and captured shrimp, crabs and other arthropods. Diseases of aquatic organisms, 27(3): 215-225.

Lo C.-F., Ho C.-H., Chen C.-H., Liu K., Chiu Y., Yeh P., Peng S., Hsu H., Liu H., Chang C. (1997). Detection and tissue tropism of white spot syndrome baculovirus (WSBV) in captured brooders of *Penaeus monodon* with a special emphasis on reproductive organs. Diseases of Aquatic Organisms, 30: 53-72.

Madigosky S.R., Alvarez-Hernandez X., Glass J. (1991). Lead, cadmium, and aluminum accumulation in the red swamp crayfish *Procambarus clarkii* G. collected from roadside drainage ditches in Louisiana. Archives of Environmental Contamination and Toxicology, 20(2): 253-258.

Nishikimi M., Rao N.A., Yagi K. (1972). The occurrence of superoxide anion in the reaction of reduced phenazine methosulfate and molecular oxygen. Biochemical and Biophysical Research Communications, 46(2): 849-854.

OIE (2003). White spot disease. In: OIE (Ed.). OIE manual of diagnostic tests for aquatic animals. OIE, Paris, 285-297

Olive P.L., Banáth J.P., Durand R.E. (1990). Detection of etoposide resistance by measuring DNA damage in individual Chinese hamster cells. Journal of the National Cancer Institute, 82(9): 779-783.

Paglia D.E., Valentine W.N. (1967). Studies on the quantitative and qualitative characterization of erythrocyte glutathione peroxidase. The Journal of Laboratory and Clinical Medicine, 70(1): 158-169.

Ramos-Carreño S., valencia-Yáñez R., Correa-Sandoval F., Ruíz-García N., Díaz-Herrera F., Giffard-Mena I. (2014). White spot syndrome virus (WSSV) infection in shrimp (*Litopenaeus vannamei*) exposed to low and high salinity. Archives of Virology, 159: 2213-2222.

Richman L.K., Montali R.J., Nichols D.K., Lightner D.V.

(1997). A newly recognized fatal baculovirus infection in freshwater crayfish. Proceedings of the American Association of Zoo Veterinarians.

Rodríguez J., Ruiz J., Maldonado M., Echeverría F. (2012). Immunodetection of hemocytes, peneidins and α2-macroglobulin in the lymphoid organ of white spot syndrome virus infected shrimp. Microbiology and Immunology, 56(8): 562-571.

Sablok G., Sánchez-Paz A., Wu X., Ranjan J., Kuo J., Bulla I. (2012). Genome dynamics in three different geographical isolates of white spot syndrome virus (WSSV). Archives of Virology, 157(12): 2357-2362.

Sahtout A.H., Hassan M., Shariff M. (2001). DNA fragmentation, an indicator of apoptosis, in cultured black tiger shrimp *Penaeus monodon* infected with white spot syndrome virus (WSSV). Diseases of Aquatic Organisms, 44(2): 155-159.

Sanchez-Zazueta E., Martinez-Cordero F.J. (2009). Economic risk assessment of a semi-intensive shrimp farm in Sinaloa, Mexico. Aquaculture Economics and Management, 13(4): 312-327.

Sánchez-Martínez J.G., Aguirre-Guzmán G., Mejía-Ruíz H. (2007). White spot syndrome virus in cultured shrimp: a review. Aquaculture Research, 38(13): 1339-1354.

Shi Z., Wang H., Zhang J., Xie Y., Li L., Chen X., Edgerton B.F., Bonami J.R. (2005). Response of crayfish, *Procambarus clarkii*, haemocytes infected by white spot syndrome virus. Journal of Fish Diseases, 28(3): 151-156.

Singh N.P., McCoy M.T., Tice R.R., Schneider E.L. (1988). A simple technique for quantitation of low levels of DNA damage in individual cells. Experimental Cell Research, 175(1): 184-191.

Sriram M.I., Kanth S.B.M.; Kalishwaralal K., Gurunathan S. (2010). Antitumor activity of silver nanoparticles in Dalton's lymphoma ascites tumor model. International Journal of Nanomedicine, 5(1): 753-762.

Tan L., Soon S., Lee K., Shariff M., Hassan M., Omar A. (2001). Quantitative analysis of an experimental white spot syndrome virus (WSSV) infection in *Penaeus monodon* Fabricius using competitive polymerase chain reaction. Journal of Fish Diseases, 24(6): 315-323.

van Hulten M.C., Witteveldt J., Peters S., Kloosterboer N., Tarchini R., Fiers M., Sandbrink H., Lankhorst R.K., Vlak J.M. (2001). The white spot syndrome virus DNA genome sequence. Virology, 286(1): 7-22.

Vlak J.M., Bonami J.R., Flegel T.W., Kou G.H., Lightner D.V., Loh C.F., Walker P.C. (2005). Family Nimaviridae, genus *Whispovirus*. Virus taxonomy, 8th reportof the International Committee on Taxonomy of Viruses. London, United Kingdom, Elsevier/Academic Press. 1162 p.

Wang S., Zhao X.-F., Wang J.-X. (2009). Molecular cloning and characterization of the translationally controlled tumor protein from *Fenneropenaeus chinensis*. Molecular Biology Reports, 36(7): 1683-1693.

Wang Y., Hassan M., Shariff M., Zamri S., Chen X. (1999). Histopathology and cytopathology of white spot syndrome virus (WSSV) in cultured *Penaeus monodon* from peninsular Malaysia with emphasis on pathogenesis and the mechanism of white spot formation. Diseases of Aquatic Organisms, 39(1): 1-11.

Witteveldt J., Vlak J. (2004). Virus-host interactions of white spot syndrome virus. In: K.Y. Leung (Ed.). Current Trends in the Study of Bacterial and Viral Fish and Shrimp Diseases. pp: 237-255.

Zeng Y., Lu C.-P. (2009). Identification of differentially expressed genes in haemocytes of the crayfish (*Procambarus clarkii*) infected with white spot syndrome virus by suppression subtractive hybridization and cDNA microarrays. Fish and Shellfish Immunology, 26(4): 646-650.

Zhu Y., Gao G. (2008). ZAP-mediated mRNA degradation. RNA Biology, 5(2): 65-67.

Zou H.S., Juan C.C., Chen S.C., Wang H.Y., Lee C.Y. (2003). Dopaminergic regulation of crustacean hyperglycemic hormone and glucose levels in the hemolymph of the crayfish *Procambarus clarkii*. Journal of Experimental Zoology Part A: Comparative Experimental Biology, 298(1): 44-52.